Freeze-Fracture Analysis of the Membrane Lesion of Human Complement

JØRGEN TRANUM-JENSEN and SUCHARIT BHAKDI
Anatomy Department C, University of Copenhagen, Panum Institute, Copenhagen, Denmark; and Institute of Medical Microbiology, Giessen, Federal Republic of Germany

ABSTRACT The structure and membrane insertion of the human C5b-9(m) complex, generated by lysis of antibody-coated sheep erythrocytes with whole human serum under conditions where high numbers of classical ring-shaped lesions form, were studied in single and complementary freeze-fracture replicas prepared by unidirectional and rotary shadowing.

The intramembrane portion of the C5b-9(m) cylinder was seen on EF-faces as an elevated, circular structure. In nonetched fractures it appeared as a solid stub; in etched fractures a central pit confirmed the existence of a central, water-filled pore in the molecule. Complementary replicas showed that each EF-face ring corresponded to a hole in the lipid plateau of the PF-face. Etched fractures of proteolytically stripped membranes revealed the extramembrane annulus of the C5b-9(m) cylinder on ES-faces and putative internal openings on PS-faces. Allowing for the measured thickness of deposited Pt/C, the dimensions of EF-face rings and ES-face annuli conformed to anticipations derived from negatively stained preparations.

Our results support the concept that the hollow cylindrical C5b-9(m) complex penetrates into the inner leaflet of the target erythrocyte membrane bilayer, forming a stable transmembrane protein channel.

Cytolysis by complement is effected by a macromolecular protein entity, the C5b-9(m) complex, which is formed through the sequential assembly on a target membrane of the terminal five complement components (3, 23, 25). The assembly occurs spontaneously on a target membrane in fresh, whole serum once the C5b fragment of the fifth component is formed upon activation of the complement system via the antibody-dependent or the alternative pathway (28, 31).

The human C5b-9(m) complex has been morphologically identified by methods of negative staining as a thin-walled cylinder, 15 nm high, with an internal diameter of 10 nm and rimmed by an annulus at one end (43). The classical, ultrastructural complement lesion (10, 21) is identical to axial projections of the C5b-9(m) cylinder on a target membrane. Apolar domains are exposed on the outer surface of the cylinder at the end opposite the annulus, enabling its insertion and stable binding within the apolar matrix of a lipid bilayer (4, 6). By comparison of the dimensions of detergent-solubilized versus membrane-inserted complexes, the depth of insertion was estimated to be 4–5 nm, and the existence of a transmembrane protein channel was suggested (4). However, negatively stained preparations do not visualize the intramembrane portion of the protein complex, and the inferred depth of insertion was not corroborated by earlier freeze-fracture studies that failed to detect penetration into the cytoplasmic leaflet of the target membrane (1, 22). The discrepancy between estimates of the functional pore size (11, 26, 40, 41) and measurements of pore size in negative stainings further urged us to obtain structural data on the complement lesion independent of negative staining.

To reinvestigate the problem, we performed a freeze-fracture analysis of the complement lesion in the classical system of antibody-coated sheep erythrocytes lysed with fresh human serum under conditions where high numbers of the classical ultrastructural lesions are generated. Rotary-shadowed complementary replicas demonstrated that C5b-9(m) complexes extend as hollow cylinders into the inner lipid monolayer of target membranes. Our results provide further evidence for the concept that insertion of C5b-9(m) creates a stable, water-filled, transmembrane channel that is believed to be the prime membrane lesion of complement.

MATERIALS AND METHODS

Sheep blood was drawn into an equal volume of Alsevers solution (72 mM NaCl, 27 mM tri-sodium citrate, 2.6 mM citric acid, and 104 mM glucose, pH 6.2), cooled to 4°C, and used within 24 h.

THE JOURNAL OF CELL BIOLOGY · VOLUME 97 SEPTEMBER 1983 618-626
 · 0021-9525/83/09/0618/09 $1.00

3 g of loosely packed erythrocytes, washed four times in 150 mM NaCl containing 5 mM sodium phosphate buffer, pH 7.2, was suspended in 15 ml of Pillemers veronal-buffered saline (5 mM sodium-veronal buffer, 145 mM NaCl, 0.5 mM $MgCl_2$, and 0.15 mM $CaCl_2$, pH 7.3). Rabbit anti-sheep erythrocyte antiserum (Amboceptor 1:6,000, Behringwerke, Marburg, Federal Republic of Germany), diluted in Pillemers buffer (350 μl of antiserum to 15 ml of buffer) was added to the stirred cell suspension. The mixture was stirred for 15–18 h at 4°C. After addition of another 50 μl of antiserum diluted in 5 ml of the same buffer, the mixture was warmed to 37.5°C for 30 min prior to lysis.

Human cubital vein blood was drawn into centrifuge tubes, left to clot at room temperature for 30 min, and then centrifuged at 4°C. A volume of 40 ml of serum was heated to 37.5°C and immediately added to the stirred erythrocyte suspension. Lysis was complete within 1 min. The resulting suspension of complement-lysed erythrocytes was then processed for freeze-fracture following the three different protocols described below.

(*a*) FRESH-FROZEN, UNFIXED PREPARATIONS: 3 min after lysis, the membrane suspension was cooled on ice and centrifuged at 0°C (RC2B centrifuge, SS-34 rotor [E. I. Dupont de Nemours & Co., Inc., Sorvall Instruments Div., Newtown, CT], 12,000 rpm, 17,400 *g*, 10 min). The packed ghosts were either frozen immediately (see below) or resuspended and washed thrice in PBS (pH 7.2) before freezing. If the cells were intended for freeze-etching the last wash was done in 5 mM sodium phosphate buffer, pH 7.2.

(*b*) FIXED PREPARATIONS: 3 min after lysis, the ghosts were washed thrice in PBS at 0°C. A volume of 0.5 ml of packed ghosts was then resuspended in 1 ml of PBS and stirred into 10 vol of ice-cold 25 mM glutaraldehyde in 0.1 M sodium phosphate buffer, pH 7.2, left at 0°C for 30 min, and pelleted. The pellets were divided into small blocks and frozen directly or after cryoprotection with glycerol in 5% increments up to 25% wt/wt over a period of 1 h. If intended for etching, the blocks were transferred to 5 mM sodium phosphate buffer, pH 7.2, before freezing.

(*c*) PROTEOLYTICALLY TREATED PREPARATIONS: Lysed cells were washed three times and resuspended to 50% cytocrit in PBS (pH 7.8). 1 vol of this suspension was added to 10 vols of a trypsin plus α-chymotrypsin solution (trypsin, Sigma type III and α-chymotrypsin, Sigma type II [Sigma Chemical Co., St. Louis, MO.] both at 0.2 mg/ml, dissolved in 50 mM sodium phosphate buffer, pH 7.8, containing 75 mM NaCl). The mixture was gently agitated at room temperature for 30 min. Then, the ghosts were sedimented at 0°C (centrifuge conditions as in *a*), washed once in PBS (pH 7.2), and resuspended to 50% cytocrit. 1 vol of this suspension was stirred into 10 vol of ice-cold 10 mM glutaraldehyde in 50 mM sodium phosphate buffer, pH 7.2, containing 75 mM NaCl, and left overnight at 0°C. The fixed ghosts were washed thrice in PBS, pH 7.2, (SS-34 rotor, 1,500 rpm, 270 *g*, 120 min, 0°C) and resuspended to 50% cytocrit. This suspension was brought to 10 vol by slow addition of 10 mM NaCl, sedimented at 1,500 rpm, and frozen without addition of glycerol.

Control Preparations

Amboceptor-coated erythrocytes were exposed to heat-inactivated serum, lysed hypotonically, and washed in 5 mM sodium phosphate buffer, pH 7.8, and subsequently processed parallel to the complement-lysed cells.

Freezing

Small blocks of fixed and pelleted cells or drops of packed suspensions were applied to standard gold plates and to double replica holders with 1-mm bore (Balzers, Hudson, NH). Specimens were frozen in freon 22 at −160°C or nitrogen slush at −210°C. Some specimens were frozen in a propane jet freezer (30) in Balzers flat sandwich holders with an intercalated gold grid. Except for trivial differences in ice crystal size, the different methods of freezing provided identical results.

Fracture and Replication

Freeze-fracture and -etching were performed in a Balzers BAF 301 unit at 10^{-7}–10^{-6} torr, −105°C (−100°C for etchings) by knife or in the double replica device. Etching periods were 30–60 s. Pt/C and C evaporations were delivered by electron guns operated at 1,800 V/60–80 mA and 2,400 V/90–110 mA, respectively. Deposited film thicknesses were measured with a quartz crystal oscillator. Degeneration of vacuum during Pt/C evaporation did not exceed 10^{-5} torr. Source-to-specimen distance was 12 cm, and specimens were either unidirectionally shadowed at 45° or rotary shadowed (1 rps) at 25° relative to the specimen table.

Replicas were floated onto water and rinsed in Sputofluol® (Merck Chemical Division, Merck & Co., Rahway, NJ) and distilled water before collection on 400-mesh naked copper grids.

For the matching of complementary replicas the two replicas were first photographed *in toto* at low (× 1625) magnification, with a photographic field corresponding to one grid square. The coordinates of each field were read on the object stage nonius of the Philips 300 electron microscope. After systematically mounting prints of these low-power micrographs, we searched for matching fractures, primarily around the replica centers. Subsequently, corresponding fracture faces were retrieved, utilizing the nonius readings, and photographed at higher magnifications.

Negative Stainings

Preparative steps were followed in negatively stained preparations, using 2% sodium silicotungstate or 2% uranyl acetate as described in reference 43. Some aliquots of the membrane preparations were fixed in 0.5% OsO_4 in 25 mM sodium phosphate buffer, pH 7.2, for 30–60 min at room temperature and washed and resuspended in distilled water before staining. Flakes of the fixed membranes were produced by forcefully drawing the suspension a few times through a fine intradermic needle.

Specimens were studied in a Philips 300 or a JEOL 100 CX electron microscope operated at 60 or 80 kV.

RESULTS

Negatively Stained Preparations

Negatively stained specimens (fixed or unfixed) were prepared of all preparations of complement-lysed membranes used for the freeze-fracture studies. OsO_4-fixed membranes are easily fragmented into flakes by shear force, permitting the survey of larger areas of single membrane layers. Problems of image interpretation due to overlay of membranes in intact ghosts are thus avoided. Glutaraldehyde or OsO_4 fixation did not produce detectable structural changes in the complement lesions.

Typical fragments of OsO_4-fixed membranes, with and without proteolytic treatment, are shown in Fig. 1, *A* and *D*. Under the experimental conditions of lysis used, most membranes displayed classical complement lesions (10, 21) at a density of 100–200 lesions/μm^2 of membrane. It is a noteworthy, but as yet unexplained, observation that all preparations contained a small fraction of membranes carrying many fewer lesions (1–10/μm^2).

Though the basic structure of the lesions was clearly that of a closed ring of ~10 nm i.d., it is relevant for the interpretation of the freeze-fractured preparations that some heterogeneity in size and shape existed. Thus, internal diameters varied within a range of 8–12 nm, and irregular forms, twinned rings, and rings with an apparent defect of closure were scattered among normal lesions (Fig. 1, *B* and *E*).

At the edges of negatively stained, intact ghosts (Fig. 1, *C* and *F*), C5b-9(m) cylinders were seen in profile, projecting ~10 nm beyond the membrane. At the site of attachment, a defect in the continuity of the light rim (representing the sharply bent edge of the ghost membrane) suggested the presence of a stain-filled, transmembrane pore (4, 43).

We did not observe any change in the structure of the C5b-9(m) complex after proteolytic treatment, but the lesions were more clearly revealed when most other membrane-bound proteins had been stripped and the lesions then tended to cluster.

Unidirectionally Shadowed, Freeze-Fracture Replicas

Fig. 2, *A* and *B*, shows the typical appearance of fracture faces EF and PF[1]) in standard, 45° unidirectionally shadowed replicas of unetched fractures of complement-lysed membranes, fixed in glutaraldehyde, and cryoprotected with glyc-

[1] The nomenclature of Branton et al., reference 12, is followed.

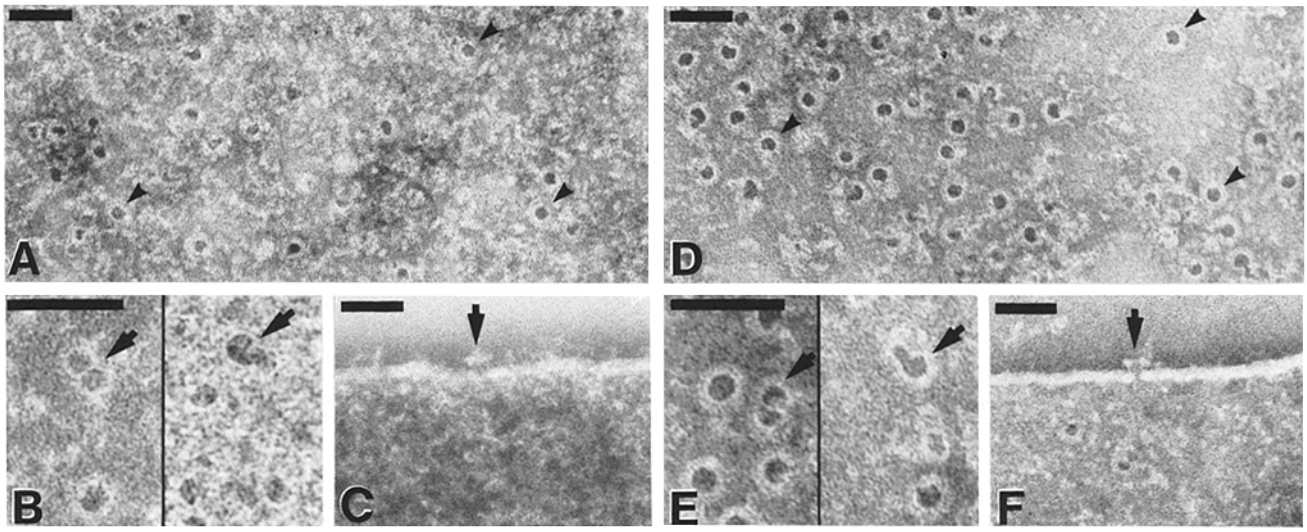

FIGURE 1 Complement-lysed membranes, fixed on OsO_4 and negatively stained with uranyl acetate (*A*) and sodium silicotungstate (*B–F*). *A–C* show membranes before—and *D–F* after—proteolytic stripping with trypsin and α-chymotrypsin. *A, B, D,* and *E* depict single-layer membrane fragments; *C* and *F* show edges of intact ghosts (two membrane layers). The classical ultrastructural complement lesions are seen as numerous, mostly circular, light rings surrounding a central stain deposit of ~10 nm diam (arrowheads, *A* and *D*). *B* and *E* show twinned and "fused" rings. *C* and *F* show lesions in profile. The existence of a stain-filled transmembrane pore, walled by the complex, is indicated by attenuation or interruption of the light rim representing the sharply bent ghost membrane. Bars, 50 nm. *A, C, D,* and *F*: × 163,000, *B* and *E*: × 295,000.

erol. Numerous flat, stub-like elevations of ~15-nm diam, with no apparent substructure, were present on the EF-faces of complement-lysed membranes, but were absent in controls. No specific structures appeared on PF-faces, except for sporadic, shallow, circular depressions in the lipid plateau. A moderate clustering of native PF-face particles was also observed regularly in control membranes.

In etched preparations (Fig. 2, *C* and *D*), the stub-like elevations on EF-faces revealed a central depression that was, however, poorly resolved and very dependent on the prevailing, local shadowing angle. By comparing the length of the shadow cast by EF-face stubs with that of the shadow cast by nearby membrane fracture edges in etched preparations (Fig. 2*C*), we estimated the height of the stubs to be about half the step height of the membrane fracture.

On PF-faces, etching resulted in the appearance of ~15-nm holes clearly detectable only when part of their circumference resided in pure lipid plateau. On the true outer membrane surfaces (ES), disclosed by etching, ring-structures were discerned (Fig. 2*D*), whereas the inner surface (PS) appeared featureless (Fig. 2*C*). We could not detect differences in EF- and PF-face lesions between fixed and unfixed, fresh-frozen and cryoprotected preparations.

Rotary-shadowed Replicas

When rotary shadowing at low (25°) angle was used, the problems of interpretation arising from local variations in the shadowing angle were largely overcome. Thus, both EF-face stubs and PF-face depressions were present with a density expected from parallel observations in negatively stained preparations. In etched fractures (Fig. 3, *A* and *B*) the EF-face lesions appeared as rings with centers devoid of platinum deposits, indicating a depression sufficiently deep to avoid deposition of platinum. On ES-faces, numerous small openings were similarly identified. On PF-faces, holes were clearly discerned.

The relationship of EF-face stubs/rings to PF-face depressions/holes was studied in rotary-shadowed complementary replicas of glutaraldehyde-fixed, cryoprotected and slightly etched membranes (Fig. 4). A total of 30 sets of complementary fracture faces were analyzed. With few exceptions, each single ring on the EF-face matched a hole on the PF-face. In those few cases where a corresponding PF-face hole was not clearly identified, the expected location was within a cluster of native membrane particles, which may have obscured the hole by deformation during fracturing.

In general, the EF-face rings were of uniform shape and size, measuring ~20 and 7 nm o.d. and i.d., respectively (Fig. 5). In the rotary-shadowed replicas, we deposited Pt/C to a thickness of 4.7 nm perpendicular to the beam at the specimen position (corresponding to 2 nm on the average specimen plane). This corresponds to a film thickness of $4.7/\pi \approx 1.5$ nm on a cylindrical surface perpendicular to the beam. Coated on both sides, the width of the rotated EF-face rings measured ~6 nm. Neglecting possible "decoration" phenomena, the approximate wall thickness of the underlying ring structure equaled 3 nm, and the inner diameter equaled ~10 nm. As in negatively stained preparations, in addition to the regular rings we observed some aberrant forms (twinned rings, rings with an apparent defect of closure, oval rings, and larger, irregular forms) (Fig. 5).

Most PF-face holes, matching EF-face rings, measured 9–13 nm, and, generally, larger rings matched larger holes. However, native integral particles located at the border of PF-face holes appeared to be capsized over the edge. It is significant that part of the circumference of PF-face holes may reside in pure lipid plateau, and that some holes were devoid of bordering membrane particles (Fig. 5).

Fracture faces of complement-lysed membranes regularly displayed fissures that were 100–200 nm long and 10–20 nm broad. By their presence on complementary fractures faces, they were identified as penetrating crevices (Fig. 4).

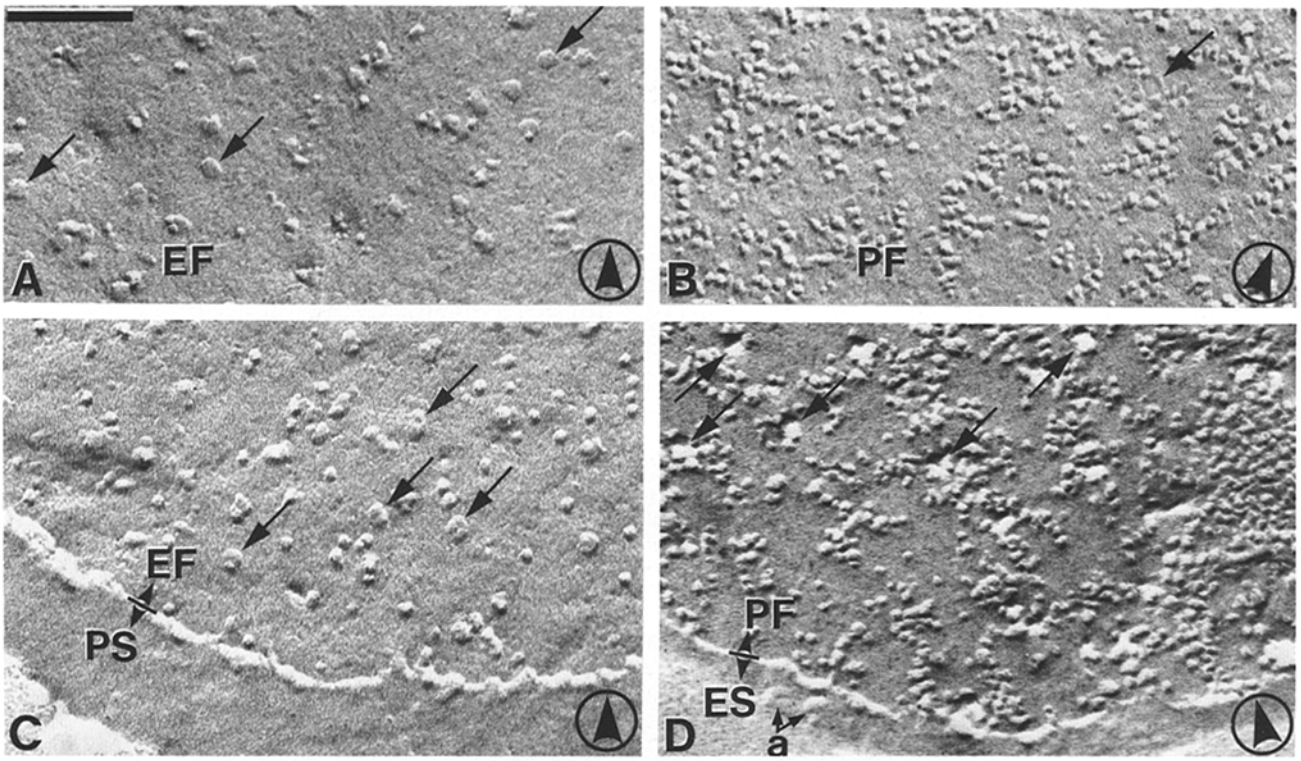

FIGURE 2 Unidirectionally shadowed freeze-fracture replicas of complement-lysed membranes. *A* and *B* derive from unetched fractures of glutaraldehyde-fixed, glycerol-cryoprotected membranes. *C* and *D* show etched fractures of unfixed, non-cryoprotected membranes. Stub-like elevations of ~15 nm diam are specific for unetched EF-faces of complement-lysed membranes (arrows, *A*), while PF-faces do not show corresponding abnormalities except for sporadic, shallow depressions (arrow, *B*). The moderate clustering of PF-face particles may be observed in controls also. However, following etching, a central depression can be discerned in the EF-face stubs, critically dependent on the shadowing angle (arrows, *C*). Etched PF-faces exhibit holes with dimensions corresponding to those of EF-face stubs (unlabeled arrows, *D*). Annular structures are discerned on ES-faces (*a*, *D*). Bar, 100 nm. × 163,000.

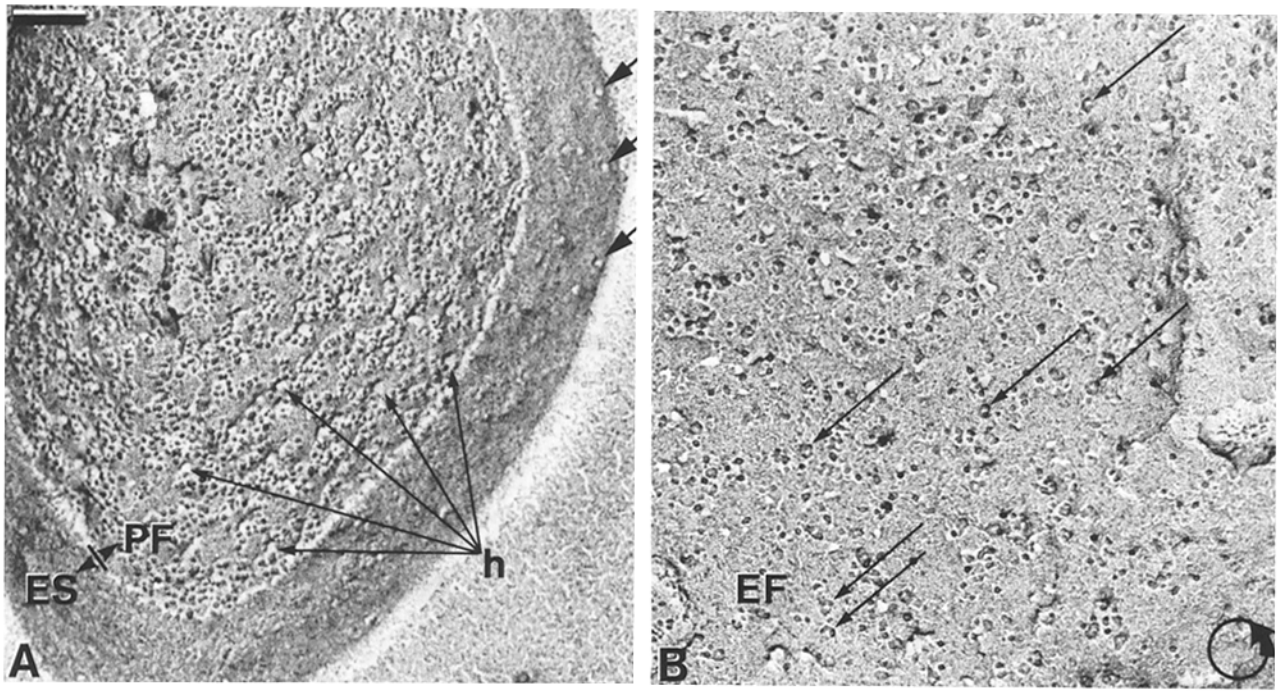

FIGURE 3 Rotary-shadowed, etched fractures of unfixed, non-cryoprotected, complement-lysed membranes. PF-faces exhibit numerous, roughly circular holes (*h*, *A*) and small openings on the ES-face (unlabeled arrows, *A*). EF-faces exhibit numerous ring-structures with centers free of platinum deposits (arrows, *B*). Bar, 100 nm. × 97,500.

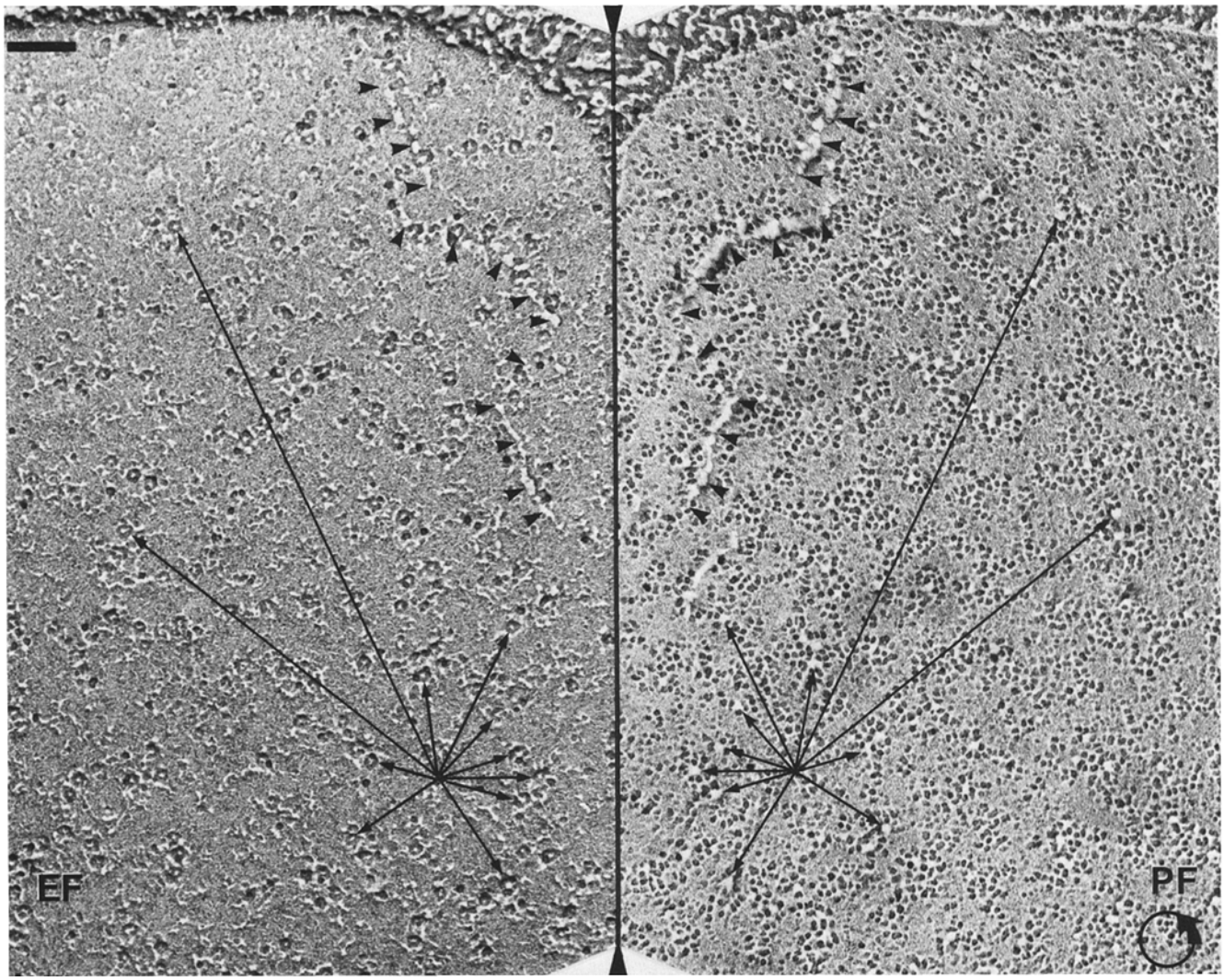

FIGURE 4 Rotary-shadowed, complementary EF- and PF-faces of glutaraldehyde-fixed, glycerol-cryoprotected and slightly etched complement-lysed membranes. EF-face rings are complementary to PF-face holes. A number of complementary pairs are indicated by "wind roses." Complementary fissures are indicated by arrowheads. Bar, 100 nm. × 97,500.

Proteolytically Treated Membranes

Consistent with observations from negatively stained preparations, the extramembrane annuli of complement lesions were visualized clearly only in preparations of proteolytically stripped membranes (Fig. 6, *A* and *C*). The external diameter of these annuli, measured in rotary-shadowed replicas and corrected for Pt/C film thickness, was 18–21 nm; internal diameters similarly corrected were 9–11 nm, in accordance with the dimensions determined after negative staining. Most ES-face annuli resided in ruffled areas continuous with areas of closely packed PF-face particles. Within or at the border of such particle aggregates, PF-face holes were present (Fig. 6, *A* and *C*). Similarly, EF-face rings on proteolysed membranes resided mostly within ruffled areas corresponding to the imprints of aggregated PF-face particles (Fig. 6*B*). The rings tended to be less regular than those seen in unproteolysed preparations, possibly due to the higher susceptibility to plastic deformation of the proteolytically "nicked" protein.

The cytoplasmic membrane surface (PS) of proteolytically stripped membranes showed ruffled areas corresponding to aggregates of intramembrane particles. Within and at the border of such areas, circular and fairly uniformly sized holes of approximately 8 nm diam were observed (Fig. 6*D*). Similar numbers of uniformly sized holes were not found on PS-faces of proteolysed control membranes.

DISCUSSION

EF-Face Lesions

We interpreted the ring structures present on etched and rotary shadowed EF-faces of complement-lysed membranes as the intramembrane portion of the hollow, cylindrical C5b-9(m) complex, based on the following arguments: (*a*) The dimensions of the rings, corrected for Pt/C film thickness, were consistent with observations on negatively stained preparations of isolated and membrane-inserted C5b-9(m) complexes (4, 43). We estimated the cylinder-wall thickness in negative staining to be 1.5 nm (noting, however, a slight thickening at the apolar terminus), whereas we found the rotary-shadowed replicas indicated a thickness of 3 nm. In view of a possible overestimate arising from "decoration" in the replicas (17, 42), and a possible underestimate owing to

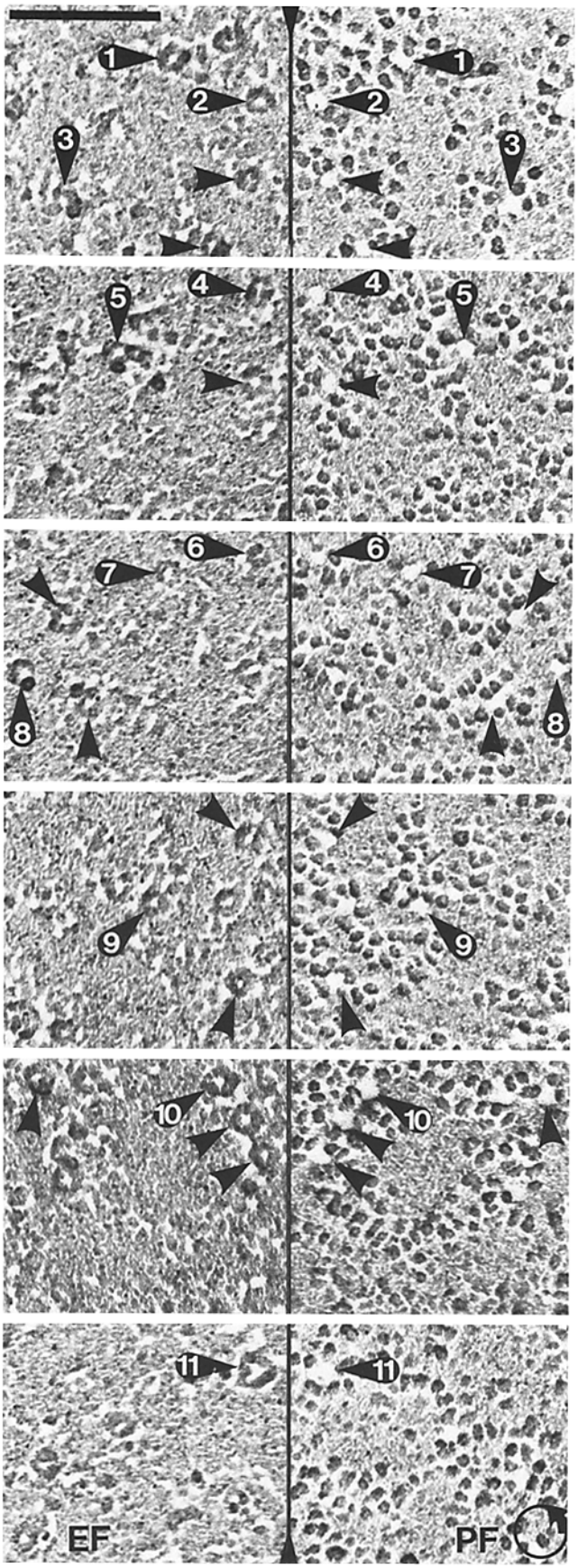

FIGURE 5 Rotary shadowed, complementary EF- and PF-faces of complement-lysed membranes, treated as in Fig. 4, showing the variability of EF-face rings and complementary PF-face holes. The

structural collapse during negative staining, the discrepancy was considered less significant than it appeared. Inner and outer diameters were fully within the range expected from negative stainings. (*b*) The apparent change of EF-face lesions from solid stubs to rings by etching indicated the existence of a central, water-filled pore, consistent with the hollow structure of the C5b-9(m) complex. Previous freeze-fracture studies have failed to recognize the EF-face lesions as distinct rings (1, 22). This is consistent with our observations on unidirectionally shadowed replicas where the clear visualization of the central pore was critically dependent on the local shadowing angle. Thus a survey of unidirectionally shadowed EF-faces could hardly establish sufficient evidence to justify the conclusion that the lesions are hollow. (*c*) In rotary-shadowed replicas, the ring structures occurred with a density fully consistent with what would be anticipated from negatively stained preparations, i.e., 100–200 lesions/μm^2 of membrane. (*d*) The EF-face rings showed some pleomorphism consistent with the aberrant forms of classical lesions observed by negative staining, allowing for some deformation during fracture (42).

PF-Face Lesions

The size of individual PF-face holes generally matched the size of corresponding EF-face rings. However, it was impossible to assess Pt/C build-up at the edges of holes vs. collapse due to undermining during etching and thermal load during shadowing. Therefore, the original size of the holes could not be deduced with precision.

Visualization of PF-face holes in unidirectionally shadowed replicas was found to be critically dependent on the shadowing angle locally in the replica, as was the case with EF-face rings.

The penetrating crevices, which were found regularly on complementary fracture faces, most likely represent the secondary lesions resulting from colloid osmotic swelling (16, 38). Owing to rapid processing after lysis, such lesions may not have completed resealing.

ES- and PS-Faces

In accordance with observations on negatively stained preparations, the extramembrane annulus of the C5b-9(m) complex was clearly visible in the etched replicas only after proteolytic treatment of the ghost membrane. This procedure also revealed a population of fairly uniform, ~8-nm holes on PS-faces. It is possible that these holes represent the internal openings of C5b-9(m) complexes.

The freeze-fracture data are compiled diagrammatically in Fig. 7. Taken together, our data provided strong evidence that the thin-walled cylindrical portion of the C5b-9(m) complex penetrates into the inner lipid monolayer. Even an incomplete

typical and consistently repeated structural unit is a regular ring with outer and inner diameters of ~20 and 7 nm on the EF-face, matching a circular hole on the PF-face, e.g., numbered pairs *2* and *9*. Some EF-face rings show an apparent defect of closure, e.g., *1* and *3*, some are larger, e.g., *10*, or irregular, e.g., *11*, while others appear small, e.g., *6* and *7*. Most rings have no apparent relation to EF-face particles, but a few are closely apposed to particles, e.g., *5* and *8*. Some rings have a tweezed appearance, e.g., *4*, which may be due to plastic deformation. The PF-face holes may reside partly, e.g., *2* and *4*, or fully, e.g., *7*, in pure lipid plateau. PF-face particles may protrude from the edges of holes, e.g., *1*. Bar, 100 nm. × 221,000.

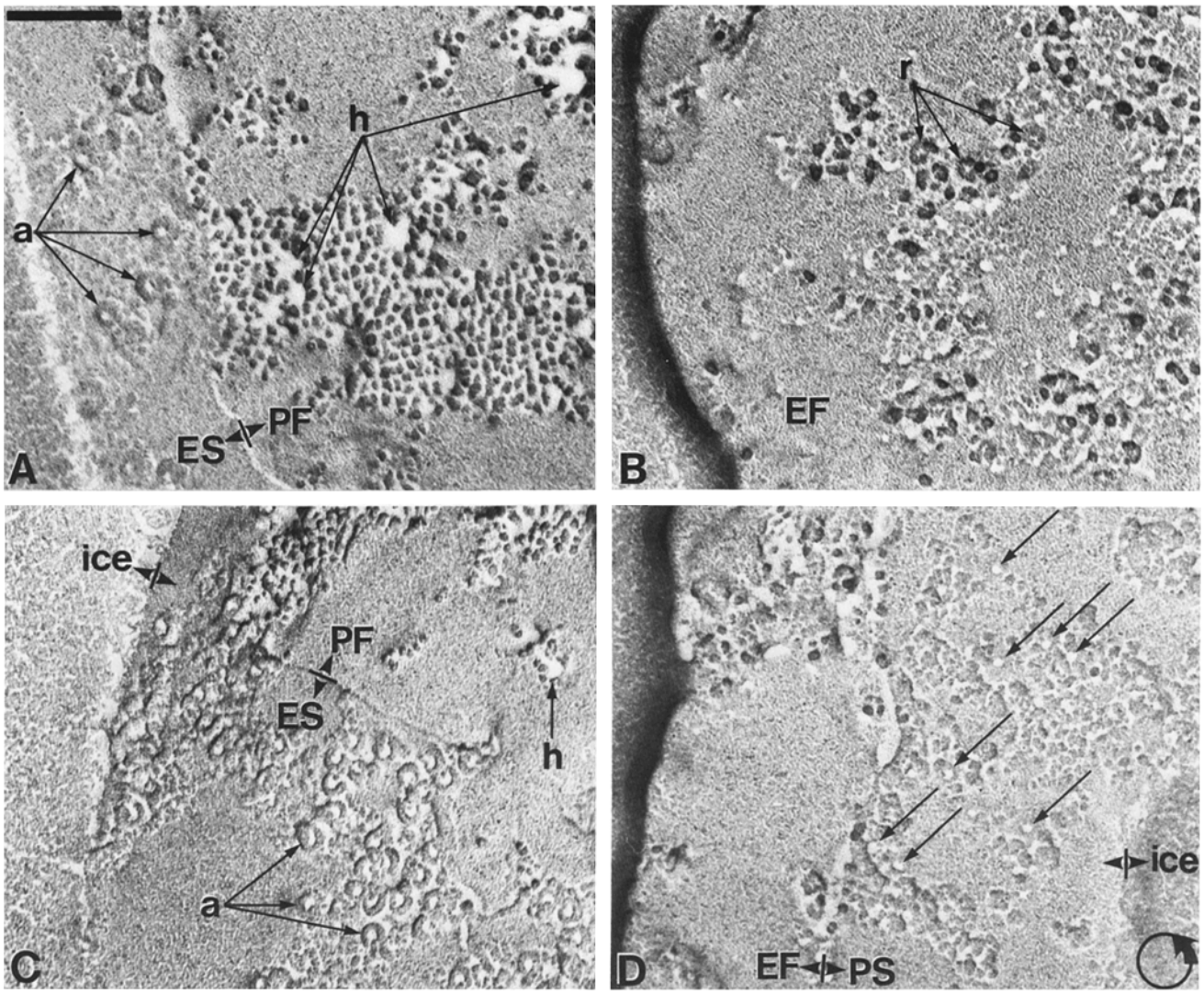

FIGURE 6 Rotary-shadowed, etched fractures of proteolytically stripped, glutaraldehyde-fixed, complement-lysed membranes. Annular structures of ~22 nm o.d. are seen on ES-faces (a, *A* and *C*). Roughly circular holes are found on PF-faces, within or at the periphery of crystal-like particle aggregates (*h*, *A* and *C*). EF-faces exhibit ring-structures similarly associated with imprints of PF-face aggregates (*r*, *B*). Fairly uniform, ~8-nm holes are found on PS-faces in relation to areas of intramembrane particle aggregation, witnessed by surface ruffling (arrows, *D*). Bar, 100 nm. × 163,000.

penetration would be likely to generate a pore in the membrane. Both negative staining and freeze-fracture observations indicated a pore diameter of ~10 nm for most lesions, and a few aberrant ("fused") complexes may produce even larger pores. However, functional and ultrastructural diameters need not be correlated.

Although it is generally accepted that the C5b-9(m) complex perturbs a target membrane by its capacity to penetrate into the hydrocarbon core of lipid bilayers through apolar interaction (2, 4, 20, 28, 33, 35, 39), opinions on the location of the functional pore are divided between a concept of disorganized lipid structure around the complex (15, 32) and a concept of a stable, water-filled channel traversing the complex (4, 27). The present data lend support to the latter concept, since the hollow structure of the C5b-9(m) complex and its penetration into the inner lipid monolayer have been confirmed independent of negative stainings, on which the morphological evidence for this model was hitherto based (4, 14, 35, 43).

While it is agreed that cytolysis by complement is effected by the C5b-9(m) complex, questions concerning the stoichiometry of the five components and their disposition in the complex are presently debated. Thus, stoichiometric compositions of $(C5b\text{-}8)_1\ C9_6$ (7, 23), $C5b\text{-}8)_2\ C9_6$ (9), and $(C5b\text{-}8)_1\ C9_{12}$ or $(C5b\text{-}8)_2\ C9_{12}$ (36) have recently been suggested. Basic to these divergencies are problems encountered in establishing a definite molecular weight for the complex; values range from one to several million as determined by hydrodynamic methods (7, 9, 45). This may partly reflect phenomena of aggregation secondary to membrane solubilization and partly a true, primary heterogeneity of composition of complexes ruled by the conditions of lysis, in particular the supply of C9 relative to C5b-8 (23, 24, 36, 45).

Indications of molecular heterogeneity also derive from functional studies. Thus, recent marker release studies on resealed ghosts have demonstrated that lesion pore sizes are critically dependent on the concentration of sensitized target membranes and the concentration of serum during lysis (13), as well as the relative input of C9 (37). These observations are in accordance with previous studies using variously sized

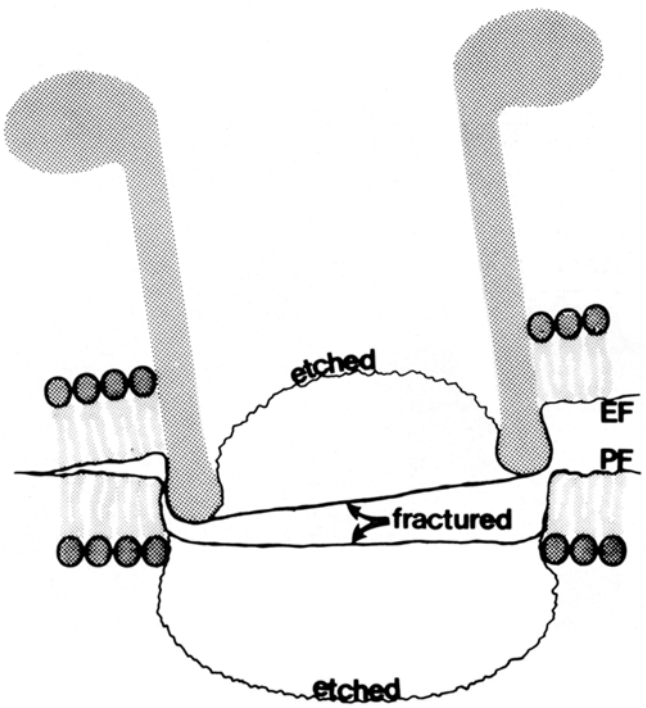

FIGURE 7 Diagrammatic presentation of the freeze-fracture behavior of a membrane-inserted C5b-9(m) complex.

osmotic blockers, indicating a broad range of functional pore sizes (11), and they offer an explanation for the small and heterogeneous pore size determined in earlier studies on steady-state diffusion under conditions of low complement input per cell (40, 41).

To sort out which stoichiometric forms and which functional pore sizes correspond to which ultrastructural lesions, precisely correlated studies need to be performed. Thus, molecular weight determinations need to be accompanied by ultrastructural characterization of individual fractions. We previously reported that the molecular weight fraction of C5b-9(m) that displays the structure of single, regular cylinders, generated under the same conditions of lysis as in the present study, has a molecular mass of $\sim 1 \times 10^6$ daltons as determined hydrodynamically (7).

Recent studies on the ability of purified C9 to polymerize have shown that C9 monomers, in the absence of C5b-8, can self-assemble in solution into a cylindrical structure that morphologically appears identical to the cylinder of the C5b-9(m) complex, indicating that C9 is the main constituent of the transmembrane protein channel (34, 36, 44). On the assumption that the cylinder structure of the C5b-9(m) complex is formed by 12–16 molecules of C9, Podack et al. (36) deduced various stoichiometric compositions of the complex from studies on the binding of labeled components in varied dosages. Thus, under conditions where numerous classical ultrastructural lesions developed, the dimeric composition $(C5b\text{-}8)_2\ C9_{12\text{-}16}$ was deduced (36). This represents a molecular mass exceeding 2×10^6 daltons. The discrepancy between this value and our earlier molecular weight estimates of $\sim 1 \times 10^6$ for the cylindrical C5b-9(m) complex (7), as well as functional data indicating a monomeric composition of the complex (37), urge precise stoichiometric determinations on morphologically defined complexes extracted from target membranes.

The studies on C9 polymerization (34, 36, 44) and experiments with apolar photolabels (20, 33) all indicate that C9 is the main constituent of the membrane-embedded portion of the cylinder. However, other components also extend into the bilayer, while still others appear mainly associated with the extramembrane annular portion of the complex (5, 8, 18, 19, 20, 29, 33). To approach the unclear details on the disposition of individual components in the C5b-9(m)complex, it will be essential to study the structure of the C5b-8(m) complex and the intermediates formed during assembly of the fully C9-saturated complex.

We gratefully acknowledge the excellent technical assistance of Ursula Hellhammer and Lisette Hansen, the skillful photographical work of Birgit Risto, and the patient secretarial assistance of Kirsten Østrem.

This work was supported by the Deutsche Forschungsgemeinschaft (grant Bh 2/1/3, 4).

Parts of this study were presented at the Ninth International Complement Workshop, Florida, 21–24 November 1981.

Received for publication 24 November 1982, and in revised form 24 May 1983.

REFERENCES

1. Bhakdi, S., V. Speth, H. Knüfermann, D. F. H. Wallach, and H. Fischer. 1974. Complement-induced changes in the core structure of sheep erythrocyte membranes: a study by freeze-etch electron microscopy. *Biochim. Biophys. Acta.* 356:300–308.
2. Bhakdi, S., O. J. Bjerrum, B. Bhakdi-Lehnen, and J. Tranum-Jensen. 1978. Complement lysis: evidence for an amphiphilic nature of the terminal membrane C5b-9 complex of human complement. *J. Immunol.* 121:2526–2532.
3. Bhakdi, S., P. Ey, and B. Bhakdi-Lehnen. 1976. Isolation of the terminal complement complex from target sheep erythrocyte membranes. *Biochim. Biophys. Acta.* 419:445–457.
4. Bhakdi, S., and J. Tranum-Jensen. 1978. Molecular nature of the complement lesion. *Proc. Natl. Acad. Sci. USA.* 75:5655–5659.
5. Bhakdi, S., and J. Tranum-Jensen. 1979. Evidence for a two-domain structure of the terminal membrane C5b-9 complex of human complement. *Proc. Natl. Acad. Sci. USA.* 76:5872–5876.
6. Bhakdi, S., and J. Tranum-Jensen. 1980. Re-incorporation of the terminal C5b-9 complement complex into lipid bilayers: formation and stability of reconstituted liposomes. *Immunology.* 41:737–742.
7. Bhakdi, S., and J. Tranum-Jensen. 1981. Molecular weight of the membrane C5b-9 complex of human complement: characterization of the terminal complex as a C5b-9 monomer. *Proc. Natl. Acad. Sci USA.* 78:1818–1822.
8. Bhakdi, S., J. Tranum-Jensen, and O. Klump. 1980. The terminal membrane C5b-9 complex of human complement. Evidence for the existence of multiple protease-resistent polypeptides that form the trans-membrane complement channel. *J. Immunol.* 124:2451–2457.
9. Biesecker, G., E. R. Podack, C. A. Halverson, and H. J. Müller-Eberhard. 1979. C5b-9 Dimer: isolation from complement lysed cells and ultrastructural identification with complement-dependent membrane lesions. *J. Exp. Med.* 149:448–458.
10. Borsos, T., R. R. Dourmashkin, and J. H. Humphrey. 1964. Lesions in erythrocyte membranes caused by immune hemolysis. *Nature (Lond.).* 202:251–252.
11. Boyle, M. D. P., A. P. Gee, and T. Borsos. 1979. Studies on the terminal stages of immune hemolysis. VI. Osmotic blockers of differing Stokes' radii detect complement-induced transmembrane channels of differing size. *J. Immunol.* 123:77–82.
12. Branton, D., S. Bullivant, N. B. Gilula, M. J. Karnovsky, H. Moor, K. Mühlenthaler, D. H. Northcote, L. Packer, B. Satir, P. Satir, V. Speth, L. A. Staehelin, R. L. Steere, and R. S. Weinstein. 1975. Freeze-etching nomenclature. *Science (Wash. DC).* 190:54–56.
13. Dalmasso, A. P., and B. A. Benson. 1981. Lesions of different functional size produced by human and guinea pig complement in sheep red cell membranes. *J. Immunol.* 127:2214–2218.
14. Dourmashkin, R. R. 1978. The structural events associated with the attachment of complement components to cell membranes in reactive lysis. *Immunology* 35:205–212.
15. Esser, A. F., W. P. Kolb, E. R. Podack, and H. J. Müller-Eberhard. 1979. Molecular reorganization of lipid bilayers by complement: a possible mechanism for membranolysis. *Proc. Natl. Acad. Sci. USA.* 76:1410–1414.
16. Green, H., P. Barrow, and B. Goldberg. 1959. Effect of antibody and complement on permeability control in ascites tumor cells and erythrocytes. *J. Exp. Med.* 110:699–713.
17. Gross, H., O. Kuebler, E. Bas, and H. Moor. 1978. Decoration of specific sites on freeze-fractured membranes. *J. Cell Biol.* 79:646–656.
18. Hammer, C. H., A. Nicholson, and M. M. Mayer. 1975. On the mechanism of cytolysis by complement: evidence on insertion of C5b and C7 subunits of the C5b, 6, 7 complex into phospholipid bilayers of erythrocyte membranes. *Proc. Natl. Acad. Sci. USA.* 72:5076–5080.
19. Hammer, C. H., M. L. Shin, A. S. Abramovitz, and M. M. Mayer. 1977. On the mechanism of cell membrane damage by complement: evidence on insertion of polypeptide chains from C8 and C9 into the lipid bilayer of erythrocytes. *J. Immunol.* 119:1–8.
20. Hu, V. W., A. F. Esser, E. R. Podack, and B. J. Wisnieski. 1981. The membrane attack mechanism of complement: photolabeling reveals insertion of terminal proteins into target membrane. *J. Immunol.* 127:380–386.
21. Humphrey, J. H., and R. R. Dourmashkin. 1969. The lesions in cell membranes caused

by complement. *Adv. Immunol.* 11:75–115.
22. Iles, G. H., P. Seeman, D. Naylor, and B. Cinader. 1973. Membrane lesions in immune lysis. Surface rings, globule aggregates, and transient openings. *J. Cell Biol.* 56:528–539.
23. Kolb, W. P., J. A. Haxby, C. M. Arroyave, and H. J. Müller-Eberhard. 1972. Molecular analysis of the membrane attack mechanism of complement. *J. Exp. Med.* 135:549–566.
24. Kolb, W. P., and H. J. Müller-Eberhard. 1974. Mode of action of human C9: adsorption of multiple C9 molecules to cell-bound C8. *J. Immunol.* 113:479–488.
25. Lachmann, P. J., and R. A. Thompson. 1970. Reactive lysis: the complement-mediated lysis of unsensitized cells. *J. Exp. Med.* 131:643–657.
26. Li, C. K. N., and R. P. Levine. 1980. Molecular transport via the functional complement lesion. *Mol. Immunol.* 17:1465–1474.
27. Mayer, M. M. 1972. Mechanism of cytolysis by complement. *Proc. Natl. Acad. Sci. USA.* 69:2954–2958.
28. Mayer, M. M. 1978. Complement, past and present. *Harvey Lect.* 72:139–193.
29. Michaels, D. W., A. S. Abramovitz, C. H. Hammer, and M. M. Mayer. 1976. Increased ion permeability of planar lipid bilayer membranes after treatment with the C5b-9 cytolytic attack mechanism of complement. *Proc. Natl. Acad. Sci. USA.* 73:2852–2856.
30. Müller, M., N. Meister, and H. Moor. 1980. Freezing in a propane jet and its application in freeze-fracturing. *Mikroskopie.* 36:129–140.
31. Müller-Eberhard, H. J. 1975. Complement. *Annu. Rev. Biochem.* 44:697–724.
32. Podack, E. R., G. Biesecker, and H. J. Müller-Eberhard. 1979. Membrane attack complex of complement: generation of high-affinity phospholipid binding sites by fusion of five hydrophilic plasma proteins. *Proc. Natl. Acad. Sci. USA.* 76:897–901.
33. Podack, E. R., W. Stoffel, A. F. Esser, and H. J. Müller-Eberhard. 1981. Membrane attack complex of complement: distribution of subunits between the hydrocarbon phase of target membranes and water. *Proc. Natl. Acad. Sci. USA.* 78:4544–4548.
34. Podack, E. R., and J. Tschopp. 1982. Polymerization of the ninth component of complement (C9): formation of poly(C9) with a tubular ultrastructure resembling the membrane attack complex of complement. *Proc. Natl. Acad. Sci. USA.* 79:574–578.
35. Podack, E. R., H. J. Müller-Eberhard, H. Horst, and W. Hoppe. 1982. Membrane attack complex of complement (MAC): three-dimensional analysis of MAC-phospholipid vesicle recombinants. *J. Immunol.* 128:2353–2357.
36. Podack, E. R., J. Tschopp, and H. J. Müller-Eberhard. 1982. Molecular organization of C9 within the membrane attack complex of complement. Induction of circular C9 polymerization by the C5b-8 assembly. *J. Exp. Med.* 156:268–282.
37. Ramm, L. E., M. B. Whitlow, and M. M. Mayer. 1982. Transmembrane channel formation by complement: functional analysis of the number of C5b6, C7, C8, and C9 molecules required for a single channel. *Proc. Natl. Acad. Sci. USA.* 79:4751–4755.
38. Sears, D. A., R. I. Weed, and S. N. Swisher. 1964. Differences in the mechanism of in vitro immune hemolysis related to antibody specificity. *J. Clin. Invest.* 43:975–985.
39. Shin, M. L., W. A. Paznekas, A. S. Abramovitz, and M. M. Mayer. 1977. On the mechanism of membrane damage by C: exposure of hydrophobic sites on activated C proteins. *J. Immunol.* 119:1358–1364.
40. Sims, P. J., and P. K. Lauf. 1978. Steady-state analysis of tracer exchange across the C5b-9 complement lesion in a biological membrane. *Proc. Natl. Acad. Sci. USA.* 75:5669–5673.
41. Sims, P. J., and P. K. Lauf. 1980. Analysis of solute diffusion across the C5b-9 membrane lesion of complement: evidence that individual C5b-9 complexes do not function as discrete, uniform pores. *J. Immunol.* 125:2617–2625.
42. Sleytr, U. B., and A. W. Robards. 1982. Understanding the artefact problem in freeze-fracture replication: a review. *J. Microsc. (Oxf.).* 126:101–122.
43. Tranum-Jensen, J., S. Bhakdi, B. Bhakdi-Lehnen, O. J. Bjerrum, and V. Speth. 1978. Complement lysis: the ultrastructure and orientation of the C5b-9 complex on target sheep erythrocyte membranes. *Scand. J. Immunol.* 7:45–56.
44. Tschopp, J., H. J. Müller-Eberhard, and E. R. Podack. 1982. Formation of transmembrane tubules by spontaneous polymerization of the hydrophilic complement protein C9. *Nature (Lond.).* 298:534–538.
45. Ware, C. F., R. A. Wetsel, and W. P. Kolb. 1981. Physico-chemical characterization of fluid phase (SC5b-9) and membrane derived (MC5b-9) attack complexes of human complement purified by immunoadsorbent affinity chromatography or selective detergent extraction. *Mol. Immunol.* 18:521–531.